

Supplementary Information

A live bacteria SERS platform for in situ monitoring of nitric oxide release from single MRSA

Zhijun Zhang,^a Xuemei Han,^a Zhimin Wang,^a Zhe Yang,^a Wenmin Zhang,^{a,b} Juan Li,^b
Huanghao Yang,^b Xing Yi Ling,^a and Bengang Xing^{*a,b}

^a Division of Chemistry and Biological Chemistry, School of Physical & Mathematical Sciences, Nanyang Technological University, Singapore, 637371, Singapore.

^b College of Chemistry, Fuzhou University, Fuzhou, Fujian, 350116, China.

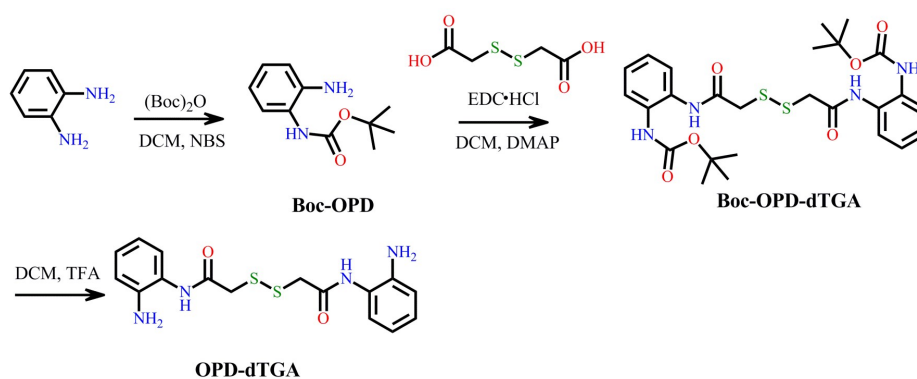
*Corresponding author: E-mail, Bengang@ntu.edu.sg

General Information

All the chemicals were purchased from Sigma Aldrich. Commercially available reagents were used without further purification. ¹H NMR and ¹³C NMR spectra were recorded using a Bruker Avance 300 spectrometer. Mass spectra (MS) were measured with Thermo Finnigan MAT 95 XP mass spectrometer for electrospray ionization mass spectra (ESI). Flash column chromatography was performed using Merck silica gel with distilled solvents. UV-visible spectra were taken with Cary 100 Bio UV-visible spectrophotometer, Agilent Technology, USA. The particle size and Zeta potential was measured using the Malvern Particles Analyser. Transmission electron microscope (TEM) images were recorded using a FEI EM208S TEM (Philips). Scanning electron microscope (SEM) imaging was performed using JEOL-JSM-7600F microscope with an EDS detector. Elements analysis was recorded on an Agilent 7700 Inductively Coupled Plasma Optical Emission Spectrometry (ICP-OES). N₂ adsorption-desorption isotherms were recorded on a Micromeritics ASAP 2020M automated sorption analyzer.

Experimental section

Probe synthesis:



Scheme S1. Synthetic route for the probe .

N-Boc-1,2-phenylenediamine (**Boc-OPD**): The compound was synthesized according to reported procedure.¹ Briefly, to a stirred solution of o-diaminobenzene (216mg, 2mmol) and Di-tert-butyl dicarbonate ($(\text{Boc})_2\text{O}$) (436mg, 2mmol) in dichloromethane (DCM) (2 mL) was added with N-bromosuccinimide (NBS) (35. mg, 0.2 mmol). After

continuously stirring at room temperature for 30 min, the solvent was removed under reduced pressure. The residue was purified by silica gel column chromatography (5-10% ethyl acetate in hexane) to get a yellowish product (yield 78%). ¹H NMR (300 MHz, CDCl₃) δ 7.29 (d, *J* = 8.3 Hz, 1H), 7.02 (td, *J* = 7.6, 1.5 Hz, 1H), 6.90 – 6.72 (m, 2H), 6.23 (s, 1H), 3.75 (s, 2H), 1.53 (s, 9H). ESI-MS: calcd for C₁₁H₁₇N₂O₂⁺ ([M+H]⁺): 209.13, found: 208.82.

di-tert-butyl(((2,2'-disulfanediy)bis(acetyl))bis(azanediyl))bis(2,1-phenylene))dicarbamate (**Boc-OPD-dTGA**): To a mixture of dithiodiglycolic acid (**dTGA**) (91 mg, 0.5 mmol), N-Boc-1,2-phenylenediamine (208mg, 1 mmol), N-(3-Dimethylaminopropyl)-N'-ethylcarbodiimide hydrochloride (EDC·HCl) (1.2 mmol) and 4-(Dimethylamino)pyridine (DMAP) (1.5 mmol) a 6 mL of DCM was added. The solution was stirred at room temperature for 24 h. After removing of the solvent under reduced pressure, the residue was added with water, and extracted with ethyl acetate. The combined organic extracts were washed with brine and dried with anhydrous Na₂SO₄. The concentrated crude product was purified by silica gel column chromatography (10-35% ethyl acetate in hexane) to afford a yellowish product (yield 81%). ¹H NMR (300 MHz, CDCl₃) δ 9.08 (s, 2H), 7.52 (dd, *J* = 15.3, 7.8 Hz, 4H), 7.26 – 6.93 (m, 6H), 3.65 (d, *J* = 2.1 Hz, 4H), 1.52 (d, *J* = 0.8 Hz, 18H). ESI-MS: calcd for C₂₆H₃₅N₄O₆S₂⁺ ([M+H]⁺): 563.20, found: 562.90.

2,2'-disulfanediy)bis(N-(2-aminophenyl)acetamide) (**OPD-dTGA**): Boc protected benzamides (112mg, 0.2 mmol) was dissolved in DCM (1 ml) and cooled with ice bath. Trifluoroacetic acid (152 μL, 2 mmol) in 200 μL DCM was added. After stirring at room temperature for 3 hr, the organic solvent was evaporated. Then ethyl acetate was added, and the residual trifluoroacetic acid (TFA) was dried with high vacuum. The resulting yellow solid was partitioned between ethyl acetate and saturated aqueous sodium bicarbonate. The organic layer was washed with brine, dried over sodium sulfate, filtered, and evaporated. The crude product was purified by column chromatography (0% - 3% methanol in DCM) to give the compound 2,2'-disulfanediy)bis(N-(2-aminophenyl)acetamide) as a white solid in 65% yield. ¹H

NMR (300 MHz, DMSO) δ 9.36 (s, 2H), 7.18 (d, $J = 7.8$ Hz, 2H), 6.92 (dd, $J = 10.9$, 4.4 Hz, 2H), 6.73 (dd, $J = 7.9$, 1.2 Hz, 2H), 6.61 – 6.45 (m, 2H), 4.89 (s, 4H), 3.76 (s, 4H). ^{13}C NMR (75 MHz, DMSO) δ 167.34, 142.53, 126.71, 126.02, 123.22, 116.60, 116.20, 56.50. ESI-MS: calcd for $\text{C}_{16}\text{H}_{19}\text{N}_4\text{O}_2\text{S}_2^+$ ($[\text{M}+\text{H}]^+$): 363.09, found: 363.01.

Synthesis of Silver nanoparticles (AgNPs): AgNPs were prepared according to previously reported method with a modification.² A new prepared 45 mL aqueous solution containing sodium borohydride (0.5 mM) and trisodium citrate (2 mM) was heated to 60 °C with vigorous stirring. After keep for 30 minutes, 5 mL aqueous solution containing 12.2 mM silver nitrate was added drop-wise. When the color keeps stable, the solution was adjusted to 10.5 with 0.1 M NaOH. Subsequently, the temperature heated to 90 °C, and kept for another 20 minutes. The obtained AgNPs were washed with citrate buffer for three times and stored at 4 °C.

Methicillin-resistant Staphylococcus aureus (MRSA, ATCC® BAA-44) modification: MRSA were cultured in Luria-Bertani (LB) medium at 37 °C with shaking, and were harvested at the exponential growth phase. AgNPs modified MRSA were fabricated in a two-step way: amino-functionalized mesoporous silica (mSi) coating and AgNPs electrostatic immobilization. mSi coating was performed according to the previous method with a slight modification.³ Briefly, to a 20 mL saccharose isotonic solution (10.3%) containing 3 μmol (3-aminopropyl) triethoxysilane (APTES), 56 μmol tetraethoxysilane (TEOS) and 2 mg mL^{-1} Pluronic®F-127, the harvested MRSA was added with a final bacterial optical density of 0.2 at 600 nm. After a moderate stirring for 4 h, the encapsulated MRSA were isolated and washed by centrifugation at 3000 rpm for 2 min. The obtained MRSA were then electrostatically modified with AgNPs by mixing with the 20 mL AgNPs solution and shaking for 30 min. Then the probe **OPD-dTGA** was modified through the strong interaction between the disulfide bonds and AgNPs. Briefly, **OPD-dTGA** DMSO solution (50 mM) was added to the suspension of AgNPs modified MRSA (PBS 7.2 buffer) with a final **OPD-dTGA** concentration of 1 mM and bacterial optical density of 0.2 at 600 nm. After incubation at room temperature for 30 min, the probes

immobilized MRSA were separated, washed, then dispersed in LB medium and stored at 4 °C for further use. The *Escherichia coli* K-12 was modified by the same procedures.

Bacterial viability test: The bacterial viability after AgNPs modification and further probe anchor was measured by fluorescein diacetate (FDA) - propidium iodide (PI) double staining method. Typically, 5 μL of PI stock solution (100 $\mu\text{g mL}^{-1}$ in deionized water) and 1 μL of the FDA stock solution (10 mg mL^{-1} in acetone) were added to 0.5 mL pH 7.2 PBS buffer containing bacteria with an optical density of 0.2 at 600 nm. After 30 min incubation at 37 °C, the stained bacteria were separated by centrifugation and washed with the PBS buffer twice. Then the bacteria were redispersed in PBS buffer and characterized by a confocal laser scanning microscope (ZEISS LSM 800).

Evaluation of bacterial proliferation: In an LB culture medium, MRSA and MRSA@AgNPs were inoculated respectively with the initial bacterial optical density of 0.025 at 600 nm. Then incubate the bacterial inoculated medium at 37 °C. The bacterial optical density at 600 nm was determined at intervals.

HPLC analysis: HPLC analyses were performed on a SHIMADZU LC-20AD instrument equipped with a diode array spectrophotometric detector (SPD-M20A). A Kromasil C18 column (150 \times 4.6 mm, 5 μm) was used with 50 mM ammonium acetate aqueous as solvent A and pure acetonitrile as solvent B. The solvent program was a linear gradient starting at 100% A and increasing to 80% B in 10 min, then remaining at 80% for 15 min; the flow rate was 1 ml/min. The eluent was monitored at 275 nm by a UV detector. Before HPLC analysis **OPD-dTGA** (400 μM in PBS 7.2) was incubated with a series different concentrations of NO at 37 °C for 2h at room temperature. HPLC analysis of 1 mM benzotriazole was performed to give the standard peak of the product.

SERS measurement: All the SERS measurements were performed on a Raman touch microspectrometer (Nanophoton Inc., Osaka, Japan) with 50 \times objective lens and 532

nm excitation wavelength. Before measurement, bacteria in pH 7.2 PBS buffer was dropped on a smooth silica surface and covered with a coverslip. SERS spectra were obtained through the point detection mode with 10 mW laser power and 3 s acquisition. The intensity of the SERS spectra was quantified by averaging at least 20 individual spectra. SERS images were collected using the X-y SERS imaging mode with a laser power of 0.2 mW and 2 s acquisition time.

The test of the sensitivity and selectivity of the probe towards NO: Diethylamine NONOate (DEA-NONOate) was used as a NO donor. The 50 mM stock solution was prepared by dissolving the powder in 0.01 M NaOH. For the sensitive test, different amounts of DEA-NONOate was spiked to a solution of 0.5 mL pH 7.2 PBS buffer containing **OPD-dTGA** modified MRSA with an optical density of 0.2 at 600 nm. After 30 min incubation at 37 °C, the bacteria were washed and redispersed in the PBS buffer for SERS test. The same procedures were processed for the selective test toward different reactive oxygen species (ROS). ROS with the concentrations of 6 μM were tested to compare with that of NO at 0.6 μM. Peroxynitrite (ONOO^-) was produced by the reaction between H_2O_2 and NaNO_2 . Hypochlorite anion (ClO^-) was generated by NaClO. Hydroxyl radical ($\bullet\text{OH}$) was prepared by the Fenton reaction. Superoxide anion (O_2^-) was derived from KO_2 DMSO solution. The first singlet oxygen ($^1\text{O}_2$) was prepared by NaClO reacting with H_2O_2 .

Monitoring NO generation from MRSA under the stress of antibiotics: In a 96 well plate, different concentration of the antibiotics, ampicillin or vancomycin, was added to the LB solution of MRSA with an optical density of 0.2 at 600 nm. After 8 h incubation at 37 °C, the MRSA was washed and redispersed in the PBS buffer for SERS test. For the NOS inhibition test, 1.5 mM N ω -Nitro-L-arginine methyl ester hydrochloride (L-NAME) was added before the 8 h incubation.

Monitoring NO generation from MRSA under the Polymicrobial infection model: The polymicrobial infection model was constructed by co-culture the MRSA with *Pseudomonas aeruginosa* PA01. In order to avoid confusion of MRSA identifying by PA01 under microscopy, here a filter membrane was set between the medium of

PA01 and the MRSA. The membrane can stop the mixing of PA01 with the MRSA, but allow the easy diffusion of the secretions from PA01. PA01 was co-cultured with an initial optical density of 0.5 at 600 nm. The MRSA was cultured with an optical density of 0.2 at 600 nm. After 8 h incubation at 37 °C, the MRSA was washed and redispersed in the PBS buffer for SERS test.

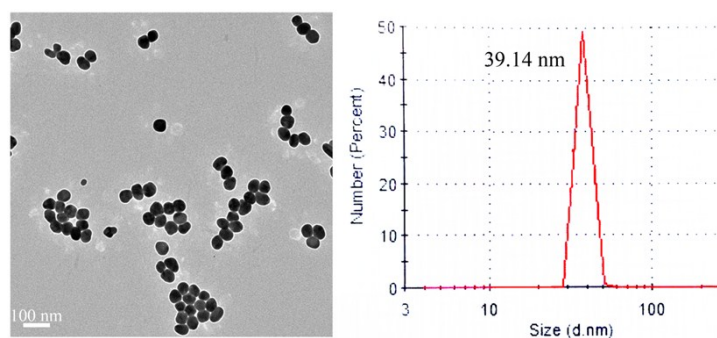


Fig. S1 TEM image and size distribution of AgNPs.

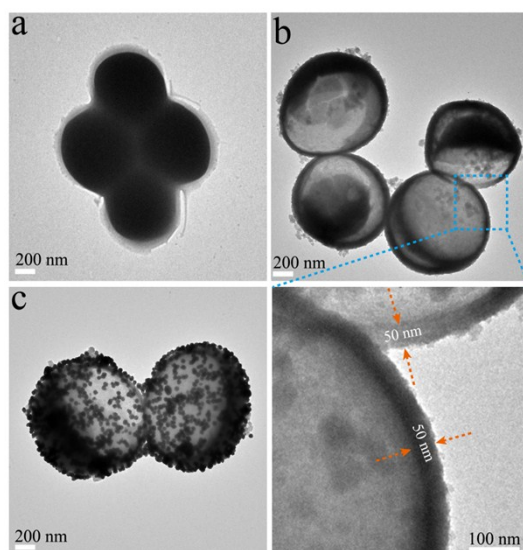


Fig. S2 TEM images of a) bare MRSA, b) mSi coated MRSA and c) AgNPs modified MRSA. The silica layer was found to be uniformly encapsulated around the bacteria with a thickness of about 50 nm.

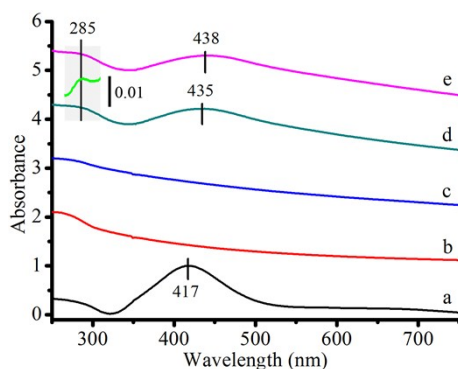


Fig. S3 UV-Vis spectra of a) AgNPs, b) MRSA, MRSA after being progressively modified with c) silica layer, d) AgNPs and e) the probe. The inserted green curve is the differential spectrum between e and d at the region around 285 nm.

As shown in Fig. S3, AgNPs exhibited a sharp surface plasmon peak at 417 nm (a). The plasmon peak of AgNPs was found to shift to 435 nm after being modified on the MRSA surface (d). The red shift was ascribed to the plasmonic coupling as nanoparticles approach each other and form some small aggregates.⁴ After probe immobilization, small shift (3 nm) on the plasmon peak of AgNPs was found, indicating that the probe immobilization didn't cause obvious status change on the AgNPs. Although there was a strong background band around 280 nm that coincides with the probe absorption spectrum (Fig. S9a, ESI[†]), the peak that was ascribed to the probe can still be observed in the differential spectrum between before and after probe immobilization (the inserted green curve).

The composition of the MRSA surface modified layer was also analyzed through inductively coupled plasma optical emission spectroscopy (ICP-OES). The sample was prepared by dissolution with dilute HNO₃ and HF. The mass ratio between Si, Ag, and S were measured to be 448:238:1. Considered the face centered cubic lattice within the silver crystal, the atoms of the silver nanoparticle (39.1 nm in diameter, Fig. S1, ESI[†]) were calculated to be 1.84×10^6 through the volume ratio. Thus, the molar ratio between the probe and silver nanoparticle was further estimated to be about 13000:1.

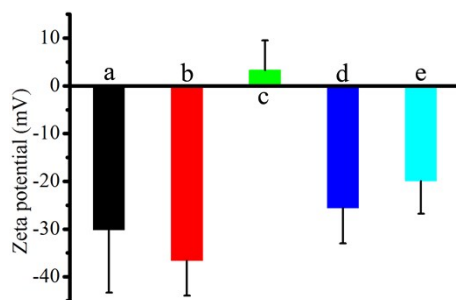


Fig. S4 Zeta potential of a) AgNPs, b) MRSA, MRSA after being progressively modified with c) silica layer, d) AgNPs and e) the probe. The data were collected in a citrate 6.0 buffer.

Both AgNPs (a) and MRSA (b) showed high negative zeta potential with the values of -30.2 and -36.6 mV respectively. After coating with the silica layer, the MRSA became positive charged with the potential of 3.3 mV due to the amino group from the silane agent (c). The zeta potential of the MRSA sharply decreased to -25.6 mV after the further modification of AgNPs through the electrostatic interaction (d). The final immobilization of the probe OPD-dTGA leads to a slightly positive shift (5.7 mV) of the zeta potential (e), which was considered to ascribe to the weak positive charge of the probe and the anchoring of the probe to AgNPs leading in a partial replacement of citrate ions.⁵

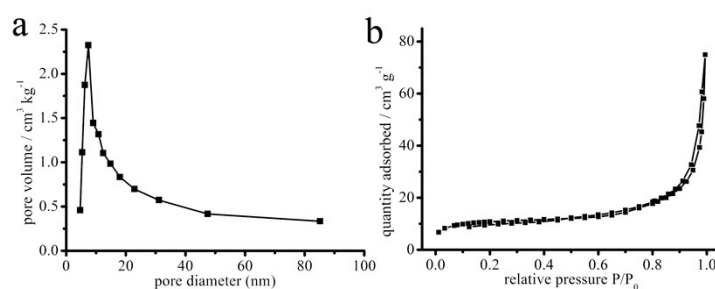


Fig. S5 BJH pore size distribution derived from the adsorption branch of the adsorption isotherm (a) and N₂ adsorption-desorption isotherms (b) of the encapsulated MRSA after calcination.

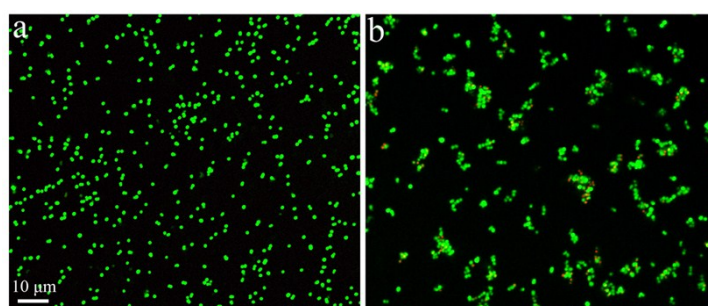


Fig. S6 Fluorescent images of FDA-PI double stained a) MRSA, b) probe modified MRSA. FDA examines the activity of intracellular esterases to generate a green fluorescence of live bacteria, while PI indicates the membrane integrity to generate a red fluorescence of dead bacteria.

Some certain aggregates were found in the fluorescence image of the modified MRSA. These aggregates may be caused by the crosslinking of the coating layer during the encapsulation, which is a very common occurrence during cell encapsulation.⁶ Fortunately, these aggregates did not affect the SERS detection in our studies.

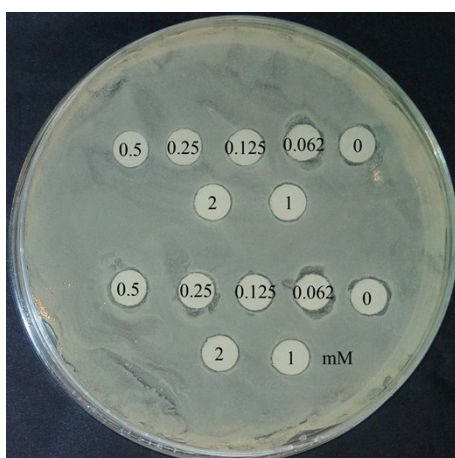


Fig. S7 Photograph of the inhibition zone by the disk diffusion assay of MRSA with the probe coated filter paper. From the picture, we can see that at the tested concentrations up to 2 mM no apparent toxicity of the probe towards MRSA was found.

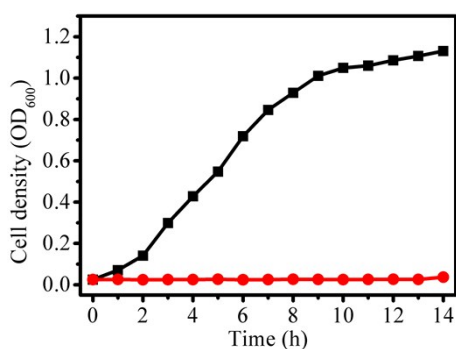


Fig. S8 Growth curve of MRSA (Black) and modified MRSA (Red).

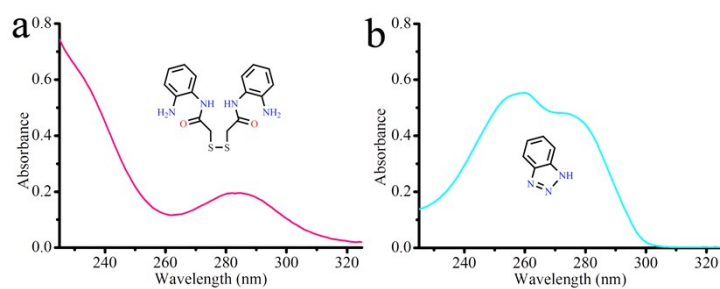


Fig. S9 UV absorption spectrum of a) **OPD-dTGA** and b) benzotriazole.

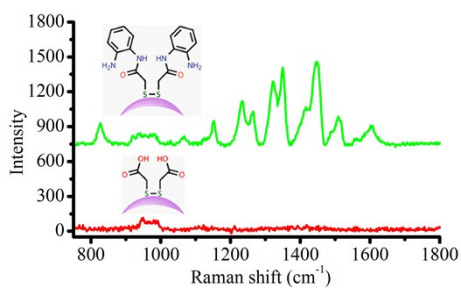


Fig. S10 SERS spectra of the probe and **dTGA**.

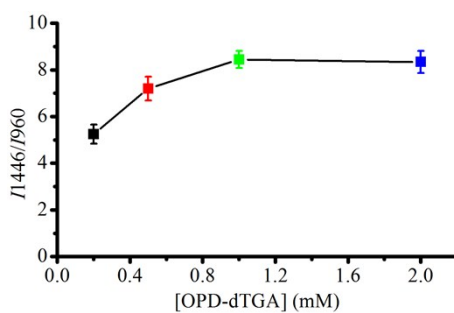


Fig. S11 The plot of I_{1446}/I_{960} as a function of **OPD-dTGA** concentration in a 30 min modification.

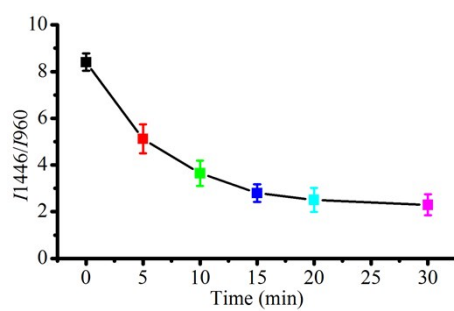


Fig. S12 The plot of I_{1446}/I_{960} as a function of the time for 1 μM of NO incubation.

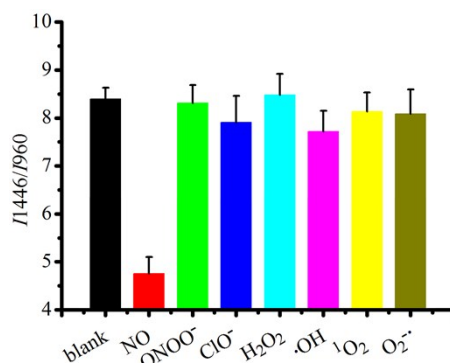


Fig. S13 SERS signal changes upon the treatment with 0.6 μM of NO and 6 μM of other different ROS ions.

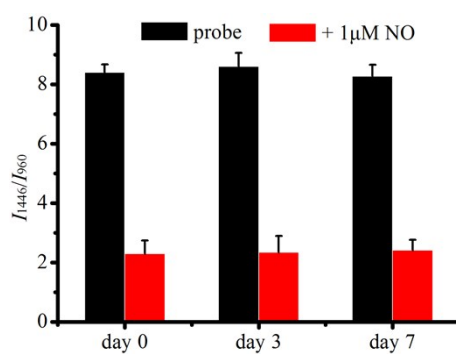


Fig. S14 SERS signal changes of the probe and that in the presence of 1 μM of NO after storage at 4 $^{\circ}\text{C}$ for the different time.

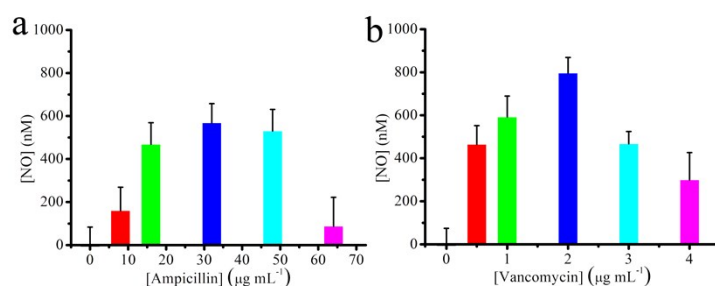


Fig. S15 NO generation in the MRSA upon exposure with different concentrations of a) Ampicillin and b) Vancomycin.

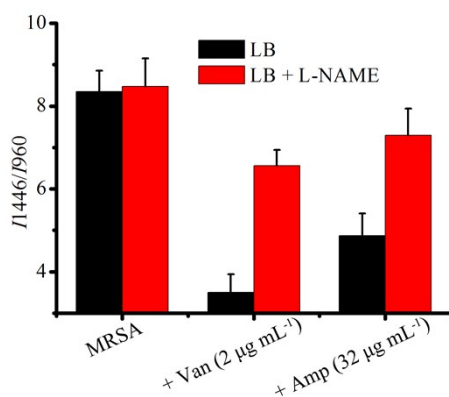


Fig. S16 SERS signal changes reflect the impact of NOS inhibitor (L-NAME) on the antibiotics induced NO generation in MRSA.

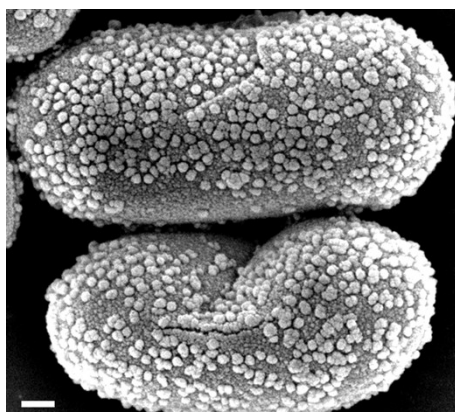


Fig. S17 SEM image of the AgNPs modified *E. coli*. Scale bar = 200 nm.

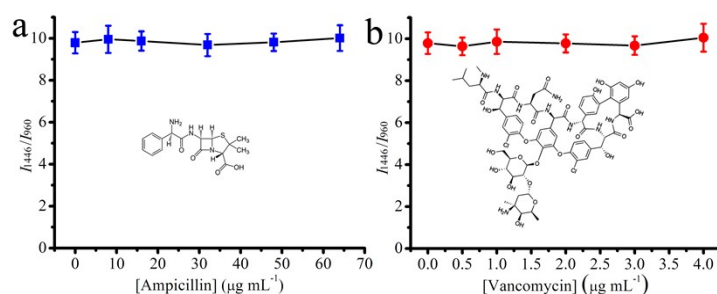


Fig. S18 SERS signal changes in the *E. coli*. K-12 upon exposure with different concentrations of a) Ampicillin and b) Vancomycin.

As shown in Fig. S18, there was no evident signal change in the Gram-negative strain *Escherichia coli* K-12 upon the antibiotics treatment, which was very different from that of MRSA. So far, many Gram-positive bacteria including *Staphylococcus aureus* have been extensively reported to produce a gene encoding nitric oxide synthase (NOS) in their chromosome.⁷ The expressed nitric oxide synthase can induce in synthesis of NO under certain stimulation. Such NOS-derived NO plays a crucial role in bacterial physiology, including bacterial virulence, infection, antibiotic resistance, and oxidative stress tolerance. However, till now, Gram-negative bacteria haven't been found to encode such gene to expression nitric oxide synthase. Therefore, the Gram-positive and -negative bacteria showed very different NO generation behavior upon antibiotics treatment.

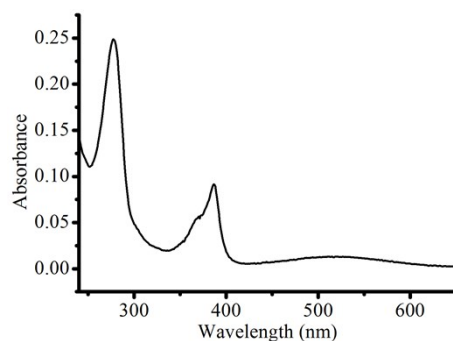


Fig. S19 UV-Vis spectrum of the pyocyanin (in 0.2 M HCl) extracted from the co-culture medium.

Reference

- 1 O. Chantarasriwong, B. Jiangchareon, C. K. Putra, W. Suwankrua and W. Chavasiri, *Tetrahedron Lett.*, 2016, **57**, 4807.
- 2 S. Agnihotri, S. Mukherji and S. Mukherji, *RSC Advances*, 2014, **4**, 3974.
- 3 Z. Zhang, E. Ju, W. Bing, Z. Wang, J. Ren and X. Qu, *Chem. Commun.*, 2017, **53**, 8415.
- 4 S. C. Hayden, G. Zhao, K. Saha, R. L. Phillips, X. Li, O. R. Miranda, V. M. Rotello, M. A. El-Sayed, I. Schmidt-Krey and U. H. F. Bunz, *J. Am. Chem. Soc.*, 2012, **134**, 6920.
- 5 (a) S. Basu, S. Pande, S. Jana, S. Bolisetty and T. Pal, *Langmuir*, 2008, **24**, 5562; (b) T. Kim, K. Lee, M.-s. Gong and S.-W. Joo, *Langmuir*, 2005, **21**, 9524; (c) N. Gandra, A. Abbas, L. Tian and S. Singamaneni, *Nano Lett.*, 2012, **12**, 2645.
- 6 (a) N. Jiang, X.-Y. Yang, Z. Deng, L. Wang, Z.-Y. Hu, G. Tian, G.-L. Ying, L. Shen, M.-X. Zhang and B.-L. Su, *Small*, 2015, **11**, 2003; (b) N. Jiang, X.-Y. Yang, G.-L. Ying, L. Shen, J. Liu, W. Geng, L.-J. Dai, S.-Y. Liu, J. Cao, G. Tian, T.-L. Sun, S.-P. Li and B.-L. Su, *Chem. Sci.*, 2015, **6**, 486; (c) Z. Chen, H. Ji, C. Zhao, E. Ju, J. Ren and X. Qu, *Angew. Chem. Int. Ed.*, 2015, **54**, 4904.
- 7 (a) I. Gusarov, K. Shatalin, M. Starodubtseva and E. Nudler, *Science*, 2009, **325**, 1380; (b) N. M. van Sorge, F. C. Beasley, I. Gusarov, D. J. Gonzalez, M. von Köckritz-Blickwede, S. Anik, A. W. Borkowski, P. C. Dorrestein, E. Nudler and V. Nizet, *J. Biol. Chem.*, 2013, **288**, 6417; (c) Jeffrey K. Holden, S. Kang, Federico C. Beasley, Maris A. Cinelli, H. Li, Saurabh G. Roy, D. Dejam, Aimee L. Edinger, V. Nizet, Richard B. Silverman and Thomas L. Poulos, *Chem. Biol.*, 2015, **22**, 785.

